Langmuir

Article

pubs.acs.org/Langmuir

Stiffness of Lipid Monolayers with Phase Coexistence

Benjamín Caruso, Agustín Mangiarotti, and Natalia Wilke*

Centro de Investigaciones en Química Biológica de Córdoba (CIQUIBIC), Departamento de Química Biológica, Facultad de Ciencias Químicas, Universidad Nacional de Córdoba, Pabellón Argentina, Ciudad Universitaria, X5000HUA Córdoba, Argentina

Supporting Information

ABSTRACT: The surface dilational modulus—or compressibility modulus—has been previously studied for monolayers composed of pure materials, where a jump in this modulus was related with the onset of percolation as a result of the establishment of a connected structure at the molecular level. In this work, we focused on monolayers composed of two components of low lateral miscibility. Our aim was to investigate the compressibility of mixed monolayers at pressures and compositions in the two-phase region of the phase diagram, in order to analyze the effect of the mechanical properties of each phase on the stiffness of the composite. In nine different systems with distinct molecular dipoles and charges, the stiffness of each phase and the texture at the plane of the monolayer were studied. In this way, we were able to analyze the general compressibility of two-phase lipid monolayers, regardless of the properties of their constituent parts. The results are discussed in the light of the following two hypotheses: first, the stiffness of the composite could be dominated by the stiffness of each phase as a weighted sum according to the percentage of each phase area, regardless of the distribution of the phases in the plane of the monolayer. Alternatively, the stiffness of the composite could be dominated by the mechanical properties of the continuous phase. Our results were better explained by this latter proposal, as in all the analyzed mixtures it was found that the mechanical properties of the percolating phase were the determining factors. The value of the compression modulus was closer to the value of the connected phase than to that of the dispersed phase, indicating that the bidimensional composites displayed mechanical properties that were related to the properties of each phases in a rather complex manner.

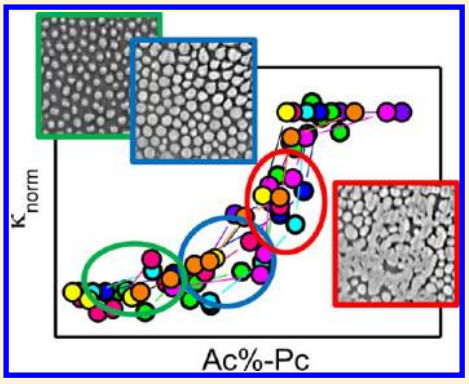

1. INTRODUCTION

Cell shape is partially encoded in the mechanical properties of the lipid bilayer, in particular the bending rigidity and the compressibility.[1] The parameter that describes the elastic behavior of surfaces under compression or expansion is the real part of the compressibility modulus κ

$$\kappa = -A\left(\frac{\partial \pi}{\partial A}\right)_T \quad (1)$$

whose definition is analogous to that of the bulk elastic modulus describing the change in surface pressure (π) resulting from a change in the total surface area (A) at constant temperature (T).

The compressibility modulus should in general be expressed as a complex number, composed of a real (elastic) and an imaginary (viscous) part, and these two components of the compressibility modulus have been measured by imposing a small-amplitude oscillatory deformation.[10,12,13] For lipid monolayers, it has been shown that, at the normally used compression rates (between 1 and 5 Å^2 molecule^{-1} min^{-1}), the imaginary part of the compressibility modulus is low.[10,12] Therefore, it can be assumed that the elastic compressibility modulus (or simply, the compressibility modulus from now on) determined using eq 1 totally characterizes the monolayer under compression. Then, using this parameter, the stiffness of these two-dimensional systems can be analyzed.

According to the Gibbs phase rule when applied to 2D systems by Crisp,[2] the lateral pressure should remain constant during the whole transition of monolayers composed of a pure lipid, and therefore, the compressibility modulus should be zero at equilibrium. In addition, as a second derivative of the surface free energy with respect to area, κ is expected to drop to zero during first-order transitions, thus defining a region of constant pressure in the compression isotherm. This property is used to corroborate the presence of phase transitions and the miscibility of components.[3,4] However, during the phase transition of pure lipids, the isotherm most generally shows a nonzero, but low, slope. This region of the isotherm (normally called "plateau") has been a highly reported observation and studied from different points of view. The first explanation given for the lack of constancy of the surface pressure during the phase transition was related with the presence of impurities[5,6] and, more recently, the presence of clusters,[7−9] kinetic effects,[10] and electrostatic repulsions have been considered.[11] Nevertheless, it is still an unresolved issue.

Received: January 9, 2013
Revised: July 18, 2013
Published: August 1, 2013

Table 1. Summary of the Analyzed Mixtures

condensed lipid	expanded lipid	subphase composition	abbreviation	analyzed lateral pressure (mN m^{-1})
dipalmitoyl phosphatidyl glycerol	dilaureyl phosphatidylcholine	Milli-Q water	DPPG/DLPC	10
distearoyl phosphatidyl glycerol	dimiristoyl phosphatidylcholine	0.15 M NaCl	DSPG/DMPC	20
dihexadecyl phosphate	dimiristoyl phosphatidylcholine	10 mM TRIS, pH 8	DHP/DMPC	10
stearic acid	dimiristoyl phosphatidylcholine	10 mM TRIS and 10 mM EDTA at pH 4	SA/DMPC, pH 4	10
stearic acid	dimiristoyl phosphatidylcholine	10 mM TRIS and 10 mM EDTA at pH 10	SA/DMPC, pH 10	40
palmitoyl ceramide	palmitoyl sphingomielyn	0.15 M NaCl	pCer/pSm	5
dipalmitoyl phosphatidylcholine	dilaureyl phosphatidylcholine	Milli-Q water	DPPC/DLPC	30
dibehenyl phosphatidylcholine	dimiristoyl phosphatidylcholine	Milli-Q water	DBPC/DMPC	20
diarachidoyl phosphatidylcholine	dimiristoyl phosphatidylcholine	Milli-Q water	DAPC/DMPC	20

The stiffness of monolayers composed of pure materials has been observed to correlate with the fractal dimension of the 2D monolayer structure, thus reflecting a link between the texture and the compressibility of the monolayer.[14,15] Risovic et al. studied the presence of defects that remain at surface pressures close to the lift-off of the isotherm. These authors established that the onset of percolation in pure lipid monolayers is characterized by the attainment of a characteristic value of the fractal dimension accompanied by a simultaneous jump in the compressibility modulus. They suggested that this observed sharp increase in the compressibility modulus at a critical point was the result of the establishment of a connected structure at a molecular level, consequently involving a change in the elastic properties of the monolayer at a macroscopic level.[14,15] However, in real systems—in technology or in biology—the surface composition is more complex, and very often nonuniform monolayers arise as a consequence of low lateral miscibility between components. Lipid membranes can in fact undergo significant density fluctuations, leading to nonuniform distributions of the chemical composition, mass density, thickness, and mechanical behavior.[16−18] Moreover, such surfaces will usually be two-dimensional dispersions with quite well-defined disperse and continuous phases. Any measurements of surface tension taken either at equilibrium or during mechanical perturbation will in general be a consequence of deformation of the continuous phase, and the question therefore needs to be addressed as to how the presence of a disperse phase affects the measured parameters and the qualitative behavior of the surface under dynamic conditions.

The response of biphasic monolayers to shear perturbations was studied using the Brownian motion of inserted particles[12,19−21] and the oscillatory motion of a magnetic needle floating at the air/water interface.[22] In all the studied systems, it was found that the presence of an increasing amount of a more rigid discontinuous phase (condensed domains) influences the effective viscosity of the continuous phase due to hydrodynamic forces and electrostatic repulsions.

Our aim was to obtain the measured stress (surface tension change) resulting from an externally applied two-dimensional strain (surface area change) on systems with two components of low lateral miscibility in order to analyze the influence of each phase on the macroscopic monolayer stiffness. While the dilational modulus can vary widely between the constituent parts of the surface, the tension should be uniform at a sufficiently small deformation rate if the effect of line tension is to be ignored.[23] We also assumed that the viscous effects were negligible.

In the present study, monolayers of nine different systems were studied, composed of two surfactants that are immiscible over a wide range of pressures and compositions. For each mixture, the phase diagram was determined from the compression isotherms of the pure and mixed monolayers and from images taken with Brewster angle microscopy. In order to analyze the change in stiffness of the composite material as it changed the amount of each phase, a pressure was selected. At this pressure, we verified that the lever rule held for each mixture, as this indicates that the phases in coexistence are the same for the whole range of global composition where the two-phases are observed and also that the lateral pressure on both phases is similar (line tension effects can be neglected).

The surfactants were chosen in order to vary the molecular dipoles and charges, the stiffness of the coexisting phases, and the distribution of the phases in the plane of the monolayer (size, shape, and density of domains). In this way, we were able to analyze general compressibility aspects of the monolayers of two surfactants with low miscibility in the region of phase coexistence. How the mechanical properties of the composites could be modulated by lipid composition was also evaluated, and an attempt was made to identify a general behavior, regardless of the composite constituent parts.

2. EXPERIMENTAL SECTION

2.1. Materials. Eight different binary lipid mixtures were selected by taking into account the stiffness of the monolayers formed by each component. One of the components formed monolayers with high values of the compressibility modulus, whereas the other had low values. All the lipids were purchased from Avanti Polar Lipids (Alabaster, AL), except dihexadecyl phosphate, which was from Sigma, and the fluorescent probe *N*-(7-nitrobenz-2-oxa-1,3-diazol-4-yl)-1,2-dihexadecanoyl-*sn*-glycero-3-phosphoethanolamine triethylammonium salt (NBD-PE) from Invitrogen, Molecular Probes. Tris-(hydroxymethyl)aminomethane (TRIS), Ethylenediaminetetraacetic acid (EDTA), and NaCl were also purchased from Sigma. The water used for the subphase was from a Milli-Q system (Millipore) with a resistivity of 18 M Ω cm and a surface tension of 72 mN/m.

Mixed monolayers were composed of the following eight couples and the indicated subphases made up the nine different analyzed systems (see Table 1):

dx.doi.org/10.1021/la4018322 | *Langmuir* 2013, 29, 10807−10816

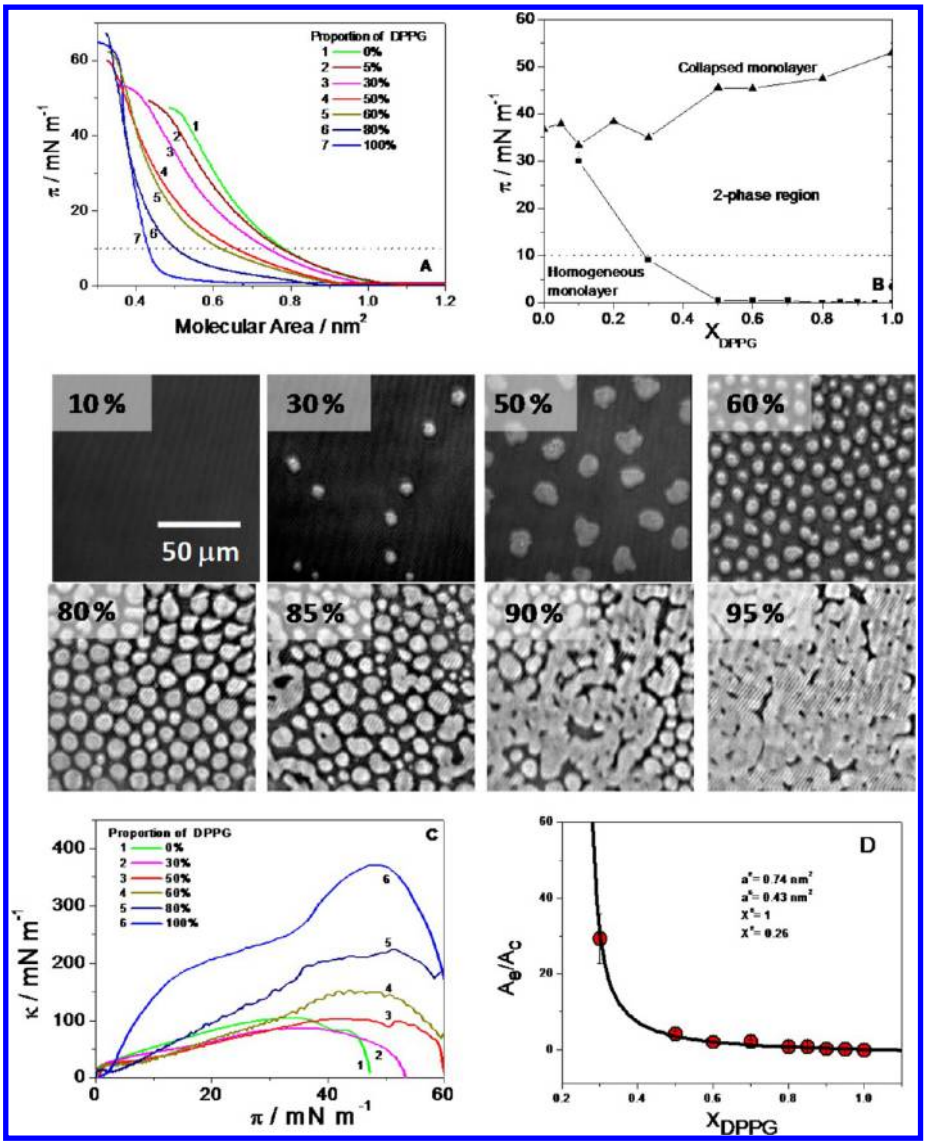

Figure 1. (A) Compression isotherms for DPPG, DLPC, and mixtures of these lipids at the indicated proportions on pure water at 21 °C. Dotted line: selected surface pressure (see the text). (B) Phase diagram of the mixture of DPPG and DLPC on pure water at 21 °C, as obtained from the isotherms and from BAM images. Dotted line: selected surface pressure (see the text). Central images: Representative BAM micrographs corresponding to the indicated proportions of DPPG at 10 mN/m. Images size: 125 μm × 125 μm. (C) Compressibility modulus as a function of the lateral pressure for the isotherms shown in part A. (D) Average ratio of the expanded area to the condensed area, taken from micrographs such as the images shown in this figure, as a function of the molar fraction of DPPG at 10 mN/m. The solid line represents the theoretical prediction according to the lever rule (eq 3) using the parameters indicated in the figure and in the text.

- Dipalmitoyl phosphatidyl glycerol with dilaureyl phosphatidylcholine (DPPG/DLPC) on pure water
- Distearoyl phosphatidyl glycerol with dimiristoyl phosphatidylcholine (DSPG/DMPC) on 0.15 M NaCl
- Dihexadecyl phosphate with dimiristoyl phosphatidylcholine (DHP/DMPC) on 10 mM TRIS, pH 8
- Stearic acid with dimiristoyl phosphatidylcholine (SA/DMPC) on subphases composed of 10 mM TRIS and 10 mM EDTA at pH 4 or 10 (The phase diagram for this mixture depends on the pH, since the compression isotherm for SA changes with the pH of the subphase.[24] Therefore, the mixture at each pH is considered as a different system.)
- Palmitoyl ceramide with palmitoyl sphingomyelin (pCer/pSm) on 0.15M NaCl
- Dipalmitoyl phosphatidylcholine with dilaureyl phosphatidylcholine (DPPC/DLPC) on pure water
- Dibehenyl phosphatidylcholine with dimiristoyl phosphatidylcholine (DBPC/DMPC) on pure water
- Diarachidoyl phosphatidylcholine with dimiristoyl phosphatidylcholine (DAPC/DMPC) on pure water

2.2. Methods. *2.2.1. Surface Pressure–Area Isotherms.* Compression isotherms at 21 ± 1 °C were carried out for each lipid mixture at different proportions. The desired composition was dissolved in chloroform:methanol (2:1) to obtain a solution of 1 nmol/μL total concentration and spread onto a KSV minitrough (KSV Instruments, Ltd. Helsinki, Finland) filled with the subphase. The initial surface area was 24 750 mm^2 and the amount of spread lipid was adjusted in order to obtain an isotherm lift-off at areas between 0.75 and 0.9 of the initial surface area. The surface pressure was determined with a Pt plate using the Wilhelmy method, and the total film area was continuously measured and recorded with a KSV apparatus (KSV, Helsinski, Finland) at rates between 1 and 5 Å^2 molecule^{-1} min^{-1}. The compression isotherms shown in Figure 1 and in the Supporting Information are representative experiments of the first compression isotherm from a set of three independent assays differing in mean molecular areas and surface pressure measurements by less than 2 Å^2

dx.doi.org/10.1021/la4018322 | *Langmuir* 2013, 29, 10807−10816

and 0.5 mN m^{-1}, respectively. In order to analyze the stiffness of the two-phase monolayers, the compressibility modulus (κ) was calculated at all surface pressures from each compression isotherm using eq 1. In spite of the fact that the isotherm appeared smooth (low noise), white noise also occurred. Since the compressibility was obtained from the derivative of the isotherms, this noise was more noticeable in the κ parameter. Smoothing algorithms were used in order to improve the representative κ plots shown in Figure 1 and in the Supporting Information, with checks continuously carried out to ensure that the original signal was not distorted by this procedure. The isotherms were smoothed using the Savitzky−Golay algorithm (polynomial order 5, window of 50−200 points), and the κ obtained from the smoothed isotherm showed less noise and the same κ value as the average κ values from the original isotherm. In the Supporting Information (Figure S1) an example is given for a curve of κ vs lateral pressure from a smoothed and a nonsmoothed isotherm.

2.2.2. Brewster Angle Microscopy (BAM) Experiments. Monolayers were spread over a Langmuir film balance in a similar manner to that described in section 2.2.1, and these were observed during compression using BAM with an EP^3 Imaging Ellipsometer (Accurion, Goettingen, Germany) with a 20× objective (Nikon, NA 0.35) and also with a 10× objective for the DBPC/DMPC mixture (Nikon, NA 0.21).

For each image acquisition, the monolayer was compressed until reaching the desired lateral pressure, and then the compression was stopped until three to five good images of different regions of the monolayer were obtained (at constant area). The image registration lasted from about 5 s to a few minutes, depending on the monolayer drift. During this time, the lateral pressure decreased by 1−2 mN/m. We determined the compression modulus from these isotherms (before stopping) and also from the isotherms determined as explained in section 2.2.1 (at constant compression) and found that the results were the same within errors. Reproducible images were also obtained, which indicated that the monolayer textures (i.e., density, size, and shape of domains) for different spread monolayers were the same within errors.

In the BAM technique, the reflected light depends on the thickness and refractive index of the lipid monolayer. When two phases are present, the condensed phase is thicker and presents a higher refractive index, therefore reflecting more light[10,15,25] and appearing lighter in the images. To determine the amount of each phase, the original gray scale images were converted to binary (black/white) images using ImageJ. Briefly, the slightly nonuniform illumination in the images (due to the intensity distribution across the laser beam profile) was discarded using a band-pass filter (or by cropping the central part of the images, with efforts always being made to analyze as large a region as possible). For each cropped image, a particular gray scale level (threshold) was selected, and all pixels with intensities above this value were converted to "black" and the pixels with intensities below this threshold level were converted to "white". The value of the threshold level was determined on the basis of an optimal resolution of the structures by constant comparison with the original photo. The detailed protocol, along with a representative example of this procedure, is shown in the Supporting Information (section S2).

Once a binary image has been obtained, the percentage of the total area occupied by the white regions was determined and named the condensed area percentage (A_c%). For a constant lateral pressure, when the global composition of the mixture in the two-phase region of the phase diagram is changed, the A_c% also changes. This change should obey the lever rule, and this was verified for each mixture.

For each image, one of the two phases was percolated (the continuous phase) and the other was discontinuous (the dispersed phase). Changes in the global composition of the mixture will change the A_c% and, eventually, invert the identity of the phase that percolates at a defined A_c% value. This particular A_c% value was named "P_c" (the percolating point of the condensed phase).

For the determination of P_c, BAM images were registered along the compression isotherms of monolayers with different compositions (varying the composition by 10 mol % or less). From these experiments, it was possible to determine at which proportions and pressures the percolating phase corresponded to the condensed phase (for the BAM resolution, which was 1 μm). The percolation threshold was at intermediate proportions, and therefore, this was determined by linear interpolation. Any errors, due to problems with reproducibility of the images in independent experiments or at different regions of the same monolayer or due to data dispersion for the determined A_c% values, were within 10% of the P_c value. An example of the procedure is detailed in the Supporting Information (section S3).

2.2.3. Fluorescence Recovery after Photobleaching (FRAP) Experiments. For the FRAP experiments, the fluorescent probe NBD-PE was incorporated into the lipid solution before spreading (2 mol %). After spreading achieved the desired surface pressure, the subphase level was reduced to a thickness of about 3 mm to minimize convection. A glass mask with lateral slits extending through the film into the subphase was used to restrict the lateral monolayer flow in the field being observed. The Langmuir film balance used for these experiments (MicroThrough, Kibron, Helsinki, Finland) was placed on the stage of an Olympus FluoView FV1000 confocal microscope. All FRAP experiments were performed with this confocal microscope using a 20× long distance air immersion objective. Bleaching was carried out using a 30 μm diameter circular bleach region (65 pixel diameter), and the region was illuminated with 488 nm (from a multiline Argon laser) at 40 mW and 405 nm (from a solid state laser) at 25 mW. The bleaching time was 5 s and the fluorescence of NBD-PE after bleaching was registered at a rate of 2 frames/s, with the gray level (GL) in a central region (7 μm diameter) of the bleached area being acquired using ImageJ. The recovery percentage was estimated by taking the GL in the central region at long times (t_∞, between 10 and 90 s), at 0.5 s after bleaching (t_{min}), and also before bleaching (t_0) as

$$\text{percentage of recovery} = \frac{GL(t_\infty) - GL(t_{min})}{GL(t_0) - GL(t_{min})} \times 100 \quad (2)$$

3. RESULTS

As detailed in section 2.1, different lipid mixtures composed of a lipid forming liquid-condensed or solid monolayers and a lipid forming liquid-expanded monolayers were analyzed. These mixtures and the corresponding subphases and abbreviations are summarized in Table 1. The mixture composed of SA and DMPC on acid and basic subphases has already been studied,[24] as well as the mixtures composed of pCer/pSm[26] and DPPC/DMPC.[27] However, to the best of our knowledge, the studies of the phase behavior of monolayers composed of the other five couples of surfactants have not been previously reported.

Below, as an example the results found for the mixture composed of DPPG and DLPC are discussed. All the information for the rest of the couples of surfactants is given in the Supporting Information. For each lipid mixture, the compression isotherms for different lipid proportions were recorded under constant conditions of temperature and subphase composition. Figure 1A show the representative compression isotherms of the DPPG/DLPC mixture at different lipid proportions. The compression isotherms were also carried out while the monolayer was being observed using BAM, and the central images in Figure 1 are from monolayers at the indicated percentage of DPPG and at 10 mN/m. These experiments allowed us to detect the regions of immiscibility of the mixtures and to be able to sketch a phase diagram for each mixture. In this way, the regions of immiscibility and the composition of the coexisting phases were determined for each system under study. Figure 1B shows the phase diagram for the DPPG/DLPC mixture.

All the studied lipid mixtures formed monolayers that had intermediate molecular area values and isotherm slopes compared with those from pure lipid monolayers. From the

compression isotherms, we calculated the compressibility modulus at all surface pressures for each lipid proportion (using eq 1), which is shown in Figure 1C for the mixtures of DPPG and DLPC.

Our aim was to analyze the variations in compressibility with respect to the proportion of the phases that coexisted in the region of the phase diagram where two phases were observed. To carry this out, the compressibility modulus was analyzed as a function of the lipid composition of the monolayer at a defined lateral pressure, since the factors that underlie variations of compressibility with composition and surface pressure are difficult to separate over the whole surface pressure range. The lateral pressure was selected by considering that at this pressure the following criteria were fulfilled: (a) There was phase coexistence over a wide range of lipid compositions, and the composition of the phases remains constant when varying the global composition (the lever rule was obeyed). (b) The selected surface pressures were not close to lift-off or to collapse. (c) The difference between the compressibility moduli of the pure lipid monolayers was as large as possible, and in this way, the κ changes associated with lipid composition variation were higher, and consequently, the relative errors were lower. (d) In the cases where the pure lipids presented phase transitions, we wanted to analyze the coexistence between the nonmiscible phases rather than the first-order phase transitions; thus, in those cases we selected for our study a lateral pressure not close to these transition points.

For the case of DPPG with DLPC, the analysis was carried out at 10 mN/m (dotted lines in Figure 1A,B). At this pressure, we calculated the ratio of the areas occupied by each phase at different lipid proportions in the region of phase coexistence, according to the phase diagram in Figure 1B for molar fractions of DPPG between a value of 0.29 and 1 (±0.03, the error derived from the preparation of the mixture from the pure lipid solutions). When the lever rule is obeyed, the experimental data should follow the trend depicted by the equation

$$\frac{A_e}{A_c} = \frac{a^e}{a^c}\frac{x^c - x}{x - x^e} \quad (3)$$

In this equation, x^e is the molar fraction of the more rigid lipid in the expanded phase and x^c is the molar fraction of the more rigid lipid in the condensed phase (both parameters being obtained from the phase diagram), while a^e is the mean molecular area of molecules in the expanded phase and a^c is the mean molecular area of molecules in the condensed phase (obtained or interpolated from the compression isotherms at the compositions x^e and x^c for the pressure under study). For the mixture formed by DPPG and DLPC at 10 mN/m and in the region of phase coexistence, Figure 1D shows the experimental data along with the curve calculated using eq 3 and $x^e = 0.26$, $x^c = 1.00$, $a^e = 0.43$ nm^2, and $x^e = 0.26$ nm^2, as these were the parameters that best fitted to the data and still corresponded to the experimental values within error (±0.03 for molar fraction and ±0.05 nm^2 for area).

Repeating the method used for the DPPG/DLPC mixture, we chose a surface pressure for the other mixtures and checked if the lever rule was obeyed. The chosen pressures were 10 mN/m for SA/DMPC (pH 4), DHP/DMPC, and DPPG/DLPC; 20 mN/m for DBPC/DMPC, DSPG/DMPC, and DAPC/DMPC; 30 mN/m for DPPC/DLPC; 40 mN/m for SA/DMPC (pH 10), and 5 mN/m for pCer/pSm (see the summary in Table 1). After determining that the lever rule was obeyed at these pressures, we analyzed the change in the compressibility modulus at this fixed pressure for different lipid proportions.

Figure 2 shows the variation in the compressibility modulus at the selected surface pressures as a function of the percentage

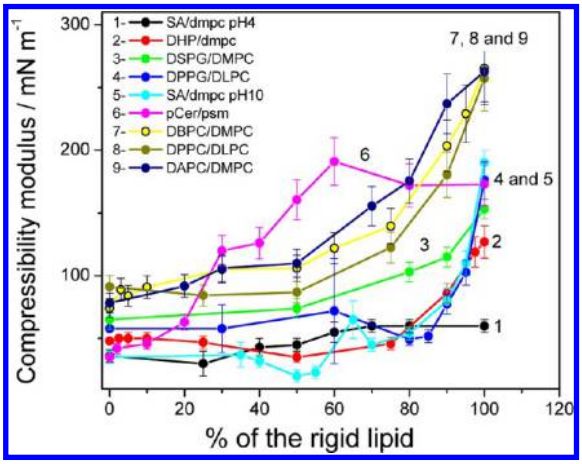

Figure 2. Compressibility modulus as a function of the mole percentage of the molecule that formed the stiffer monolayer at 10 mN/m (SA/DMPC pH 4, DHP/DMPC, and DPPG/DLPC), 20 mN/m (DBPC/DMPC, DSPG/DMPC, and DAPC/DMPC), 30 mN/m (DPPC/DLPC), 40 mN/m (SA/DMPC, pH 10), and 5 mN/m (pCer/pSm).

(in moles) of the lipid that formed the more condensed monolayer. As expected, in all cases the monolayers became stiffer as the proportion of the rigid lipid increased. Furthermore, the percentage of lipid in which the compression modules increased abruptly was different for each mixture. This result was also to be expected, since the phase diagrams of each mixture were different. For example, SA/DMPC at pH 10 and 40 mN/m remains homogeneous up to 35% of SA,[24] whereas DBPC/DMPC at 20 mN/m was segregated into two phases for DBPC proportions as low as 5% (see the phase diagram in the Supporting Information).

4. DISCUSSION

Our aim was to analyze the general compressibility aspects of monolayers of two surfactants with low miscibility in the region of phase coexistence and to evaluate how the mechanical properties of composites could be modulated by lipid composition. An attempt was made to determine a general behavior, regardless of the composite constituent parts, through a comparative analysis in order to find properties that permitted a common description of all the systems. Two possibilities relating the distribution of the phases were analyzed: First, it was considered that the stiffness of the composite came from the individual properties of each phase and that the distribution of the phases in the plane of the monolayer was not a determining factor. In other words, this implies that the resulting compressibility modulus of a two-phase monolayer was not influenced by the identity of the percolating phase nor dependent on the density, size, or shape of the island formed by the lipids in the phase state that was disconnected (these island are normally called "domains" when the disconnected phase state is the denser phase state). However, if the distribution of the phases was a determining factor for the observed monolayer stiffness, then the mechanical properties of the percolating

dx.doi.org/10.1021/la4018322 | Langmuir 2013, 29, 10807−10816

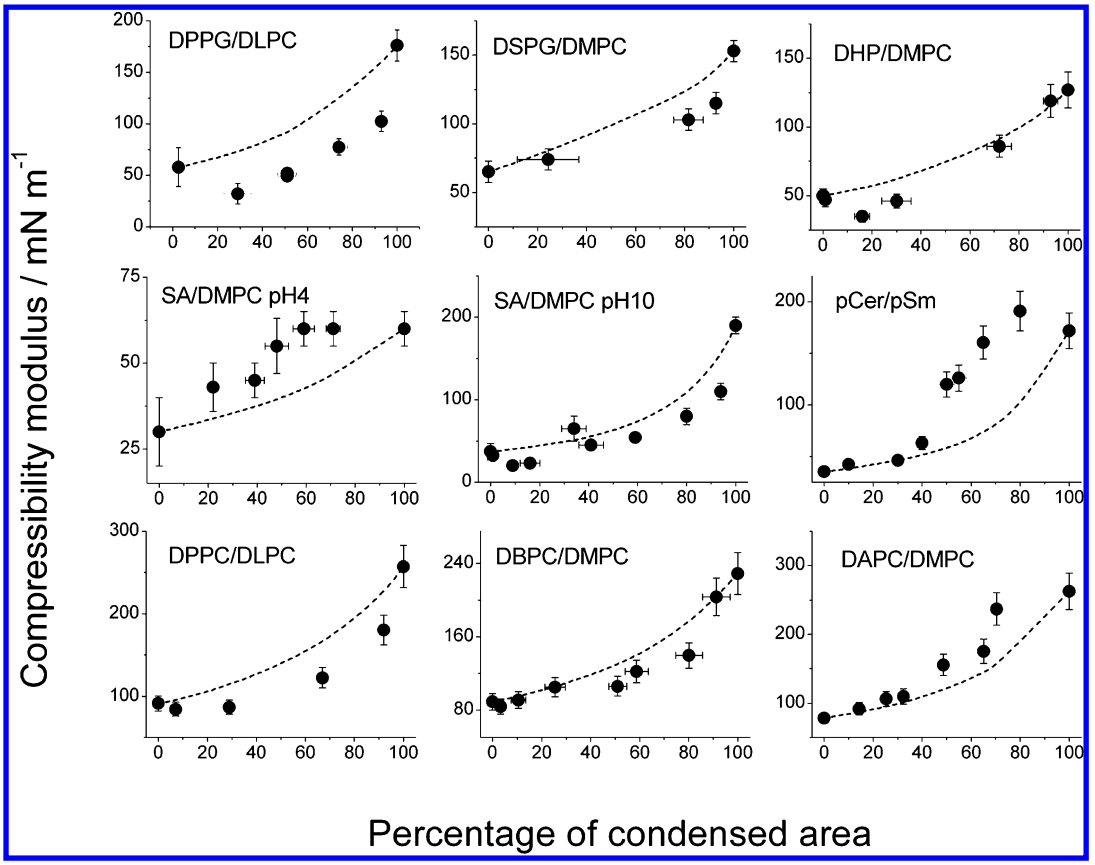

Figure 3. Compressibility modulus as a function of the percentage of condensed area calculated by using eq 4 (lines) and experimental data (dots). The surface pressures and data are the same as in Figure 2.

phase would influence the composite compressibility properties more strongly than those of the discontinuous phase.

In both these cases, the total monolayer area (A) is the sum of the area occupied by the condensed phase (A_c) and the area occupied by the expanded phase (A_e): $A = A_e + A_c$. In addition, the reciprocal of the compressibility modulus, which is the surface compressibility, is equal to $\kappa^{-1} = -(1/A)(\partial A/\partial \pi)_T$. The first hypothesis was tested in the following section and the second in section 4.2.

4.1. Compression Properties Are Not Influenced by the Manner in Which the Phases Are Distributed in the Plane of the Monolayer. In this case, the following applies:

$$\kappa^{-1} = -\frac{1}{A}\left(\frac{\partial(A_e + A_c)}{\partial \pi}\right)_T = \frac{1}{A}\left(\frac{A_e}{\kappa_e} + \frac{A_c}{\kappa_c}\right) \quad (4)$$

This derivation was made by assuming that the variation of the composition of the phases with pressure could be neglected. However, we are aware that in certain mixtures (e.g., see Figure 1 for DPPG/DLPC) the phase boundary between one- or two-phase regions of the phase diagram showed a monotonic variation with surface pressure, implying that the composition of each phase varied with surface pressure. Nevertheless, the change in phase composition did not depend on the global composition. In other words, the term in $(\partial A/\partial \pi)_T$ derived from changes in the composition of the phases with the surface pressure was constant along a line parallel to the x-axis in the phase diagram and thus did not affect our analysis and therefore will not be considered in our discussion of the results.

To test the model described, the data in Figure 2 was plotted as a function of the percentage of the area occupied by the denser phase (A_c%; symbols in Figure 3) along with the predicted trends using eq 4 (lines in Figure 3) for each mixture, with the values of A_c% being obtained as explained in section 2.2.2. Figure 3 shows that none of the nine analyzed systems followed the theoretical curve over the whole range of phase percentage. For some mixtures (DSPG/DMPC, pCer/pSm, DBPC/DMPC, and DAPC/DMPC), the curve and the data overlapped for low coverage of the condensed phase (lower than 50%). Some other mixtures (SA/DMPC pH 4, pCer/pSm, and DAPC/DMPC) presented positive deviations, whereas the rest showed negative deviations.

For the mixture formed by DPPG and DLPC, which did not show phase transitions for the pure lipid monolayers, we tested the theoretical approach at two other lateral pressures (5 and 30 mN/m). This analysis is depicted in Figure S9 (Supporting Information), where it can be observed that the trend predicted by eq 4 did not overlap with the experimental data at any of the analyzed pressures selected in three different regions of the phase diagram.

It is clear from Figures 3 and S9 (Supporting Information) that the stiffness of the two-phase monolayers over the whole range of possible compositions was not just the sum of the properties of each phase weighted by the amount of the phase with phase coexistence leading to the emergence of different properties.

4.2. Compression Properties Dominated by Those of the Phase That Percolates. Since the observed compression modulus appeared to depend not only on the proportion and properties of each phase but also on some other parameters, it is possible that the distribution of each phase in the plane of the

dx.doi.org/10.1021/la4018322 | Langmuir 2013, 29, 10807−10816

Table 2. Summary of the Properties of Each Analyzed System

system	DPPG/DLPC	DSPG/DMPC	DHP/DMPC	SA/DMPC (pH 4)	SA/DMPC (pH 10)	pCer/pSm	DPPC/DLPC	DBPC/DMPC	DAPC/DMPC
mol %[a]	93	80	87	60	95	35	97	60	80
P_c[b]	88	82	72	43	94	50	97	50	65
circularity[c]	0.80 ± 0.05	0.8 ± 0.2	0.8 ± 0.1	0.9 ± 0.1	0.8 ± 0.2	0.8 ± 0.2	0.8 ± 0.2	0.7 ± 0.2	0.9 ± 0.1

[a]Mole percentage of the stiffer component (the one that formed stiffer monolayers when pure) at the percolating point of the more condensed phase in the mixture. [b]Percentage of condensed area corresponding to the mole percentage indicated in footnote a (see the text for a further explanation of P_c). [c]Circularity (see the text) for images obtained at a 20−30 mol % lower than that indicated in footnote a.

monolayer and/or the identity of the continuous phase played a role. We therefore determined the proportion of the more rigid lipid and the corresponding percentage of the condensed area, where the identity of the phase that percolates (the continuous phase) changed. This was performed at a micrometer scale, i.e., for each system we determined the percentage of the condensed area, which when converted into a binary image (black and white, as explained in section 2.2.2) the connected phase changed from being the black (expanded) phase to the white (condensed) phase (for a detailed explanation of this procedure, see the Supporting Information, section S3). This particular condensed area percentage was named "P_c", and the corresponding values for each mixture are summarized in Table 2. Since DBPC/DMPC displayed a more heterogeneous pattern than the other mixtures, the determination of P_c was performed with a 20× objective as well as with a 10× one, leading in both cases to the same value (see below).

When the mechanical properties of the phase that percolates are dominating, the composite stiffness should change at P_c. Below this value, κ is expected to be closer to the value for the expanded phase, and above P_c, κ should be closer to the value for the condensed phase. If this were the case, the variation of the compressibility modulus with composition would not be the same in the different mixtures, since P_c did not have the same value for the series of analyzed mixtures (see Table 2). This model may justify why the deviation of eq 4 was positive for SA/DMPC pH 4, pCer/pSm, and DAPC/DMPC, since these mixtures had the lowest P_c values. Although, from this viewpoint, DBPC/DMPC should also have presented a positive deviation, which was not the case, this mixture was also an exception in the analysis presented below and will be discussed separately.

To test the above hypothesis, the compressibility moduli were normalized (the normalized parameter changed from 0 to 1 for all the mixed monolayers) to allow us to compare the nine systems. Each compression modulus was normalized according to

$$\kappa_{norm} = \left(\frac{\kappa - \kappa_0}{\kappa_{100} - \kappa_0}\right) \quad (5)$$

In this equation, κ is the compressibility modulus for a given lipid proportion (and thus condensed area), κ_0 and κ_{100} are the compressibility moduli for monolayers at the composition of each coexisting phase (for proportions at the border of the region of two phases in the phase diagram), where κ_0 is the value for the expanded phase (0% of condensed area) and κ_{100} represents the condensed phase (100% of condensed area).

This normalized compressibility was plotted as a function of the percentage of condensed area minus P_c. Figure 4 shows the trend of the nine analyzed systems, with eight of the analyzed systems following a similar behavior: the compression modulus initially increased smoothly and then changed more abruptly,

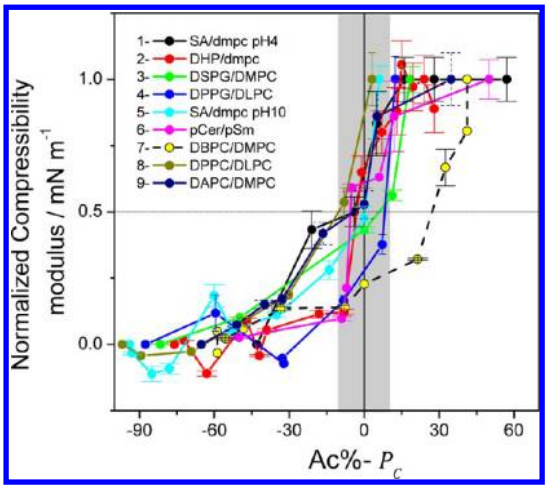

Figure 4. Normalized compressibility modulus (κ_{norm}) as a function of the percentage of condensed area (A_c) minus its percolation threshold (P_c). The surface pressures are the same as in Figure 2. The discontinuous line at κ_{norm} = 0.5 serves to guide the eye and the gray region indicates the experimental dispersion of the zero value on the *x*-axis.

reaching the value of κ_{norm} = 0.5 in the region delimited in gray in Figure 4. This gray region is the one where $A_c\% = P_c$ within errors (±10%; see section 2.2.2 and Supporting Information). Once the compressibility of the condensed area was reached, this value was maintained until the whole monolayer was in a condensed phase (homogeneous monolayer).

In an exception, the κ_{norm} value for monolayers composed of DBPC and DMPC changed abruptly only when the condensed area was about 30% larger than P_c. Another observed difference in this system was that the domain shapes were in general more elongated. For comparison, Figure 5 shows images for each mixture with a high percentage of condensed areas (close to or at the composition for the change in percolating phase, see legend).

The observed differences were quantified by the average circularity of the domains [$C = 4\pi$ area/(perimeter)^2] obtained from the binary images of monolayers with the rigid molecule at 20 or 30 mol % lower than P_c (using ImageJ). The results are summarized in Table 2. The values of circularity of all the analyzed mixtures are the same within error, with discrepancies arising from the data dispersion due to polydispersity, since not all domains in a monolayer presented the same size and shape. However, the average C value was slightly lower (0.7) for the mixture composed of DBPC and DMPC. The elongated domain shape may have given rise to rearrangements upon compression, since if domains were not strongly interconnected they could have reoriented relative to one another when the monolayer was compressed. In other words, it is possible that the domains were still not connected at P_c, which was

dx.doi.org/10.1021/la4018322 | *Langmuir* 2013, 29, 10807−10816

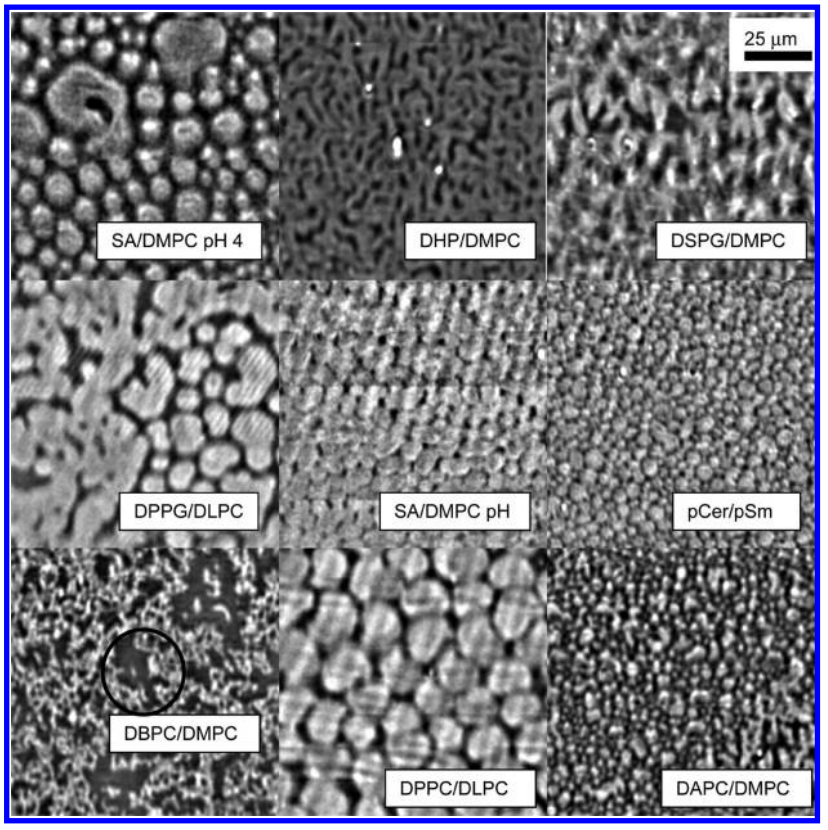

Figure 5. Representative images for the nine analyzed systems. The surface pressures and the lipid compositions are 10 mN/m and 60:40 for SA/DMPC (pH 4), 10 mN/m and 90:10 for DHP/DMPC, 20 mN/m and 80:20 for DSPG/DMPC, 10 mN/m and 90:10 for DPPG/DLPC, 40 mN/m and 95:5 for SA/DMPC (pH 10), 5 mN/m and 30:70 for pCer/pSm, 20 mN/m and 60:40 for DBPC/DMPC, 30 mN/m and 90:10 for DPPC/DLPC, and 20 mN/m and 70:30 for DAPC/DMPC. The circle in the system formed by DBPC and DMPC is an example of the photobleached regions analyzed in Figure 6.

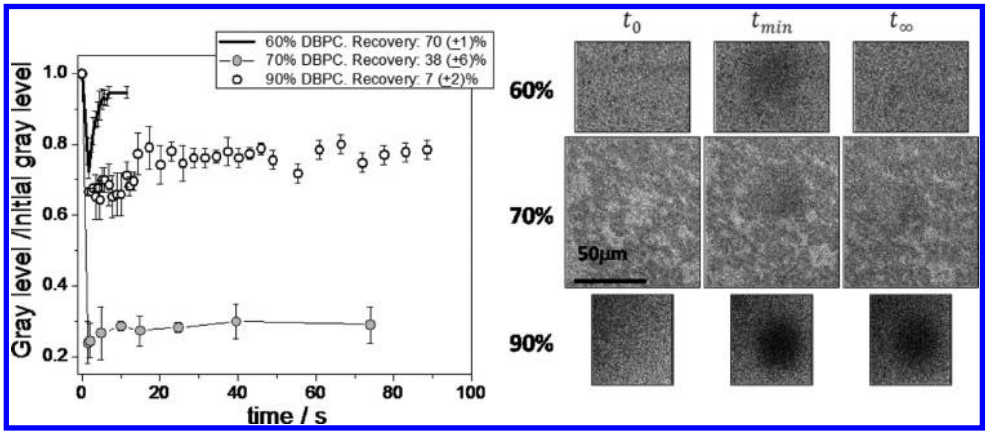

Figure 6. Left: Gray level normalized by the initial value (mean ± standard deviation of three experiments) in the region of the monolayer that was photobleached as a function of time for the mixture composed of DBPC and DMPC at the indicated lipid proportions. The percentage of recovery was calculated according to eq 2. Right: Representative images for the three lipid proportions before bleaching (t_0), immediately after bleaching (t_{min}), and after a long time (t_∞), i.e., at the longest time shown for each curve. The images were cropped and the minimum and maximum gray levels were changed from the range 0−255 to the ranges 25−160 (60 mol % DBPC), 10−150 (70 mol % DBPC), and 0−25 (90 mol % DBPC) for better viewing. The scale bar corresponds to all displayed images.

determined from the BAM images (i.e., with a micrometer scale resolution, not a molecular one).

In order to analyze the above possibility, we determined the connectivity between the expanded phase at different DBPC/DMPC proportions using fluorescence recovery after photobleaching (FRAP). In these experiments, 2% of a fluorescent-marked lipid (NBD-PE) was added, which localized at the expanded phase at a higher concentration than in the condensed phase. Therefore, when the fluorescent probe was added, the percolation occurred at higher proportions than 60 mol % of DBPC. The recovery of the fluorescence of NBD-PE in the expanded phase was tested for 60, 70, and 90 mol % of DBPC, and for 70 mol %, the molecules of NBD-PE present in corrals of the expanded phase surrounded by the condensed phase were bleached (see encircled region in Figure 5).These results are summarized in Figure 6, where the fluorescence of

dx.doi.org/10.1021/la4018322 | *Langmuir* 2013, 29, 10807−10816

the bleached region is plotted as a function of time (average of three different bleached regions of the same monolayer). For conditions under which the condensed domains were not connected (60 mol % of DBPC), 70% of the fluorescence was recovered (calculated with eq 2) in about 7 s. For 70 mol % of DBPC, the domains seemed connected in the micrograph but up to 38% of the fluorescence at the corrals was recovered in about 10 s. In other words, 70 mol % of NBD-PE diffused more slowly than 60 mol % of DBPC, but it was still able to cross the barrier that seemed to be formed by the condensed phase, thus indicating that the condensed phase was not connected at a molecular level in spite of the fact that the BAM images showed them connected. This situation might explain why the normalized compression modulus was lower than 0.5, even when it seemed percolated at the micrometer scale.

The bleaching in monolayers with 90 mol % of DBPC was performed in a region of the condensed phase, in order to study the recovery inside this phase. A very low fluorescence recovery (7%) was found, due to the diffusion of the probe in the condensed phase. This permitted us to confirm that the recovery in monolayers with 70% of DBPC could not be explained by considering only the diffusion of the probe in the condensed phase, since that was faster.

All the experiments of fluorescence recovery were carried out in order to analyze the connectivity of the phases in the DBPC/DMPC mixture rather than for quantifying the diffusion. However, an estimation of the diffusion coefficients showed that our experiments agreed with previously reported results of the diffusion of molecules in expanded and condensed monolayers (see Supporting Information, section S5).

5. CONCLUSIONS

In the present study, we have focused on the monolayer compressibility of systems with two components with low lateral miscibility in the region of the phase diagram, with the two phases being observed at the micrometer scale. Our purpose was to analyze the effect of the compression properties of each phase on composite stiffness. It was found that the monolayers did not behave as the weighted sums of each coexisting phase but, rather, that the distribution of the phases in the plane of the monolayer was a determining factor. The observed compression modulus value was closer to that of the phase that percolated than to the other phase. Thus, the degree of interconnection between each phase and its percolating point was a determining factor in the compressibility of each system.

The compression modulus increased continuously as the area occupied by the condensed phase increased, reaching the average value of the pure phases (κ_{norm} = 0.5) when the condensed phase became the continuous phase (at $A_c\% = P_c$). When the continuous phase was the expanded phase, the presence of condensed domains increased the stiffness of the monolayer. However, once the percolating phase became the condensed phase, the rigidity of the monolayer was similar to that of the condensed phase, regardless of the presence of the expanded phase in corrals formed by the condensed phase. An exception to this rule was observed for the DBPC/DMPC system, which revealed elongated domains that were still not connected at the molecular level, even though the micrograph showed a connection between them. We hypothesize that since these domains were not connected from a molecular viewpoint, they were able to reorient relative to each other when the monolayer was compressed, thereby exhibiting less stiff behavior than the condensed phase. A future challenge will be to understand the molecular aspects that hinder detection of the percolation point when using the techniques with a resolution at the micrometer scale for this particular mixture.

The effect of the presence of domains in the dilute regime (low A_c% values) was explained in some cases using the model described by eq 4; for monolayers composed of DSPG/DMPC, pCer/pSm, DBPC/DMPC, and DAPC/DMPC the curve calculated using eq 4 and the experimental data overlapped for low coverage of the condensed phase (lower than 50%). However, the rest of the mixtures did not follow the same trend for this dilute condition; therefore, a general behavior cannot be hypothesized. In this regard, from figure 4 it can be observed that the mixtures did not show the same behavior in the region of A_c% for values 20% lower than P_c, i.e., for values of the x-axis around −20. This different behavior was probably a consequence of different domain−domain interactions or differences in the shape/size of the domains between the systems. This interesting observation is currently being investigated.

In conclusion, we found that the macroscopic dilational properties of the bidimensional composites displayed emerging properties that were related to the local mechanical properties in a rather complex manner. This interplay between global and local mechanical properties may play a role in the mechanics of cell membranes under the action of lateral stress.

■ ASSOCIATED CONTENT

Supporting Information

Section S1, complete data for each mixture: (A) compression isotherms, (B) phase diagrams, (C) compressibility modulus, and (D) lever rule; section S2, convertion of an image from a scale of gray to a binary image; section S3, determination of the percolating point of the condensed phase; section S4, variation of the compressibility modulus with the percentage of condensed area at different surface pressures for DPPG/DLPC mixtures; section S5, estimation of the diffusion coefficient of the NBD-PE fluorescent probe in monolayers composed of DBPC and DMPC from the FRAP experiments. This material is available free of charge via the Internet at http://pubs.acs.org/.

■ AUTHOR INFORMATION

Corresponding Author

*E-mail: wilke@mail.fcq.unc.edu.ar. Tel/Fax: +54-351-4334171.

Notes

The authors declare no competing financial interest.

■ ACKNOWLEDGMENTS

This work was supported by SECyT-Universidad Nacional de Córdoba, Argentina, CONICET, and FONCYT (Program BID 0770), Argentina. N.W. is Career Investigator and A.M. and B.C. are fellows of CONICET. We thank Dr. Paul Hubson, a native speaker, for revision of the manuscript.

■ REFERENCES

(1) Evans, E. Structure and deformation properties of red blood cells: Concepts and quantitative methods. *Methods Enzymol.* **1989**, *173*, 3−35.

(2) Gaines, G. L. *Insoluble Monolayers at Liquid−Gas Interfaces*; Interscience Publishers: New York, 1966.

(3) Brown, R. E.; Brockman, H. L. Using monomolecular films to characterize lipid lateral interactions. *Methods Mol. Biol.* **2007**, *398*, 41−58.
(4) Smaby, J. M.; Momsen, M. M.; Brockman, H. L.; Brown, R. E. Phosphatidylcholine acyl unsaturation modulates the decrease in interfacial elasticity induced by cholesterol. *Biophys. J.* **1997**, *73* (3), 1492−1505.
(5) Pallas, N. R.; Petica, B. A. Liquid-expanded to liquid-condensed transitions in lipid monolayers at the air/water interface. *Langmuir* **1985**, *1*, 509−513.
(6) Gutberlet, T.; Vollhardt, D. Thermally induced domain growth in fatty acid ester monolayer. *J. Colloid Interface Sci.* **2013**, *173*, 429−435.
(7) Rosetti, C. M.; Wilke, N.; Maggio, B. Thermodynamic distribution functions associated to the isothermal phase transition in Langmuir monolayers. *Chem. Phys. Lett.* **2006**, *422*, 240−245.
(8) Israelachvili, J. N. Self-assembled in two dimensions: Surface micelles and domain formation in monolayers. *Langmuir* **1994**, *10* (3774), 3781.
(9) Fainerman, V. B.; Vollhardt, D. Phase transition in Langmuir monolayers. *Colloids Surf.* **2002**, *176* (117), 124.
(10) Arriaga, L. R.; Lopez-Montero, I.; Ignes-Mullol, J.; Monroy, F. Domain-growth kinetic origin of nonhorizontal phase coexistence plateaux in Langmuir monolayers: Compression rigidity of a Raft-like lipid distribution. *J. Phys. Chem. B* **2010**, *114* (13), 4509−4520.
(11) Ruckenstein, E.; Li, B. Surface equation of state for insoluble surfactant monolayers at the air/water interface. *J. Phys. Chem. B* **1998**, *102*, 981−989.
(12) Wilke, N.; Vega Mercado, F.; Maggio, B. Rheological properties of a two phase lipid monolayer at the air/water interface: Effect of the composition of the mixture. *Langmuir* **2010**, *26*, 11050−11059.
(13) Cicuta, P.; Terentjev, E. M. Viscoelasticity of a protein monolayer from anisotropic surface pressure measurements. *Eur. Phys. J. E* **2005**, *16*, 147−158.
(14) Risovic, D.; Frka, S.; Kozarac, Z. The structure of percolating lipid monolayers. *J. Colloid Interface Sci.* **2012**, *373* (1), 116−121.
(15) Risovic, D.; Frka, S.; Kozarac, Z. Application of Brewster angle microscopy and fractal analysis in investigations of compressibility of Langmuir monolayers. *J. Chem. Phys.* **2011**, *134* (2), 024701.
(16) Brown, D. A.; London, E. Structure and function of sphingolipid- and cholesterol-rich membrane rafts. *J. Biol. Chem.* **2000**, *275* (23), 17221−4.
(17) Simons, K.; Ikonen, E. Functional rafts in cell membranes. *Nature* **1997**, *387* (6633), 569−72.
(18) Engelman, D. M. Membranes are more mosaic than fluid. *Nature* **2005**, *438* (7068), 578−580.
(19) Wilke, N.; Maggio, B. The influence of domain crowding on the lateral diffusion of ceramide-enriched domains in a sphingomyelin monolayer. *J. Phys. Chem. B* **2009**, *113* (38), 12844−12851.
(20) Forstner, M.; Martin, D.; Rückerl, F.; Käs, J.; Selle, C. Attractive membrane domains control lateral diffusion. *Phys Rev E* **2008**, *77*, 051906−1−051906−7.
(21) Selle, C.; Rückerl, F.; Martin, D.; Forstner, M.; Käs, J. Measurement of diffusion in Langmuir monolayers by single-particle tracking. *Phys. Chem. Chem. Phys.* **2004**, *6*, 5535−5542.
(22) Ding, J.; Warriner, H. E.; Zasadzinski, J. A. Viscosity of two-dimensional suspensions. *Phys. Rev. Lett.* **2002**, *88* (16), 168102.
(23) Lucassen, J. Dynamic dilational properties of composite surfaces. *Colloids Surf.* **1992**, *65*, 139−149.
(24) Vega Mercado, F.; Maggio, B.; Wilke, N. Phase diagram of mixed monolayers of stearic acid and dimyristoylphosphatidylcholine. Effect of the acid ionization. *Chem Phys. Lipids* **2011**, *164*, 386−392.
(25) Vega Mercado, F.; Maggio, B.; Wilke, N. Modulation of the domain topography of biphasic monolayers of stearic acid and dimyristoyl phosphatidylcholine. *Chem. Phys. Lipids* **2012**, *165*, 232−237.
(26) Busto, J. V.; Fanani, M. L.; De, T. L.; Sot, J.; Maggio, B.; Goni, F. M.; Alonso, A. Coexistence of immiscible mixtures of palmitoyl-sphingomyelin and palmitoylceramide in monolayers and bilayers. *Biophys. J.* **2009**, *97* (10), 2717−2726.
(27) Sanchez, J.; Badia, A. Atomic force microscopy studies of lateral phase separation in mixed monolayer of dipalmitoylphosphatidylcholine and dilauroylphosphatodylcholine. *Thin Solid Films* **2003**, *440*, 223−239.